



High-resolution seismic study of the Nahal Darga fan-delta, Dead Sea, Israel, with the aim to relate the surface and subsurface tectonic structures

Y. Eyal¹, I. Bruner², G. Cadan¹, Y. Enzel³, and E. Landa²

¹Department of Geological and Environmental Sciences, Ben-Gurion university of the Negev, Beer-Sheva, 84105, Israel

²The Geophysical Institute of Israel, Lod, 71100, Israel

³Institute of Earth Sciences, the Hebrew University of Jerusalem, Jerusalem, 91904, Israel

Received: 20 November 2000 – Revised: 21 November 2001 – Accepted: 28 November 2001

Abstract. Faulting and deformation of fan-delta deposits located near active tectonic zones can be attributed either to failure due to basin-ward gravitational mass movement, or to tectonic activity. Distinguishing between these two failure mechanisms is sometimes crucial when attempting to assess the seismic risk and earthquake recurrence time of such terrains. In a case study described here, close spatial association between subsurface faults, determined in seismic profiles, and overlying surface deformation features mapped in the field, would imply tectonic activity as the cause for deformation rather than basin-ward gravitational mass movement. The geologic and seismic study of the 400 m long Nahal Darga fan-delta of Holocene age, located on the western margins of the tectonically active Dead Sea transform, is used here as a test case for this debate. The studied fan-delta is comprised of two deformation zones. The Western deformation zone consists of NNE trending normal faults with up to 2 m offsets, mostly crossing part of the section and terminating below the surface. Only a few faults cross the entire Holocene section. The Eastern zone is characterized by many small normal faults, which are restricted to only a few beds and NNE trending allochthonous bodies (slumps) that developed due to tectonic activity. A shallow, high-resolution seismic study carried out in the Nahal Darga fan-delta, reveals the existence of deep-seated faults extending up to about ten meters below the surface. The location of the subsurface faults below the surface deformation zones suggests association between the two and a tectonic origin for both. It is concluded that detailed geological and structural mapping of fan-deltas coupled with a high resolution seismic survey is an essential and reliable tool for the analysis of tectono-stratigraphy in fan-deltas.

1 Introduction

The left-lateral Dead Sea transform (DST) is an active plate boundary between the Arabian and the African plates (e.g. Freund et al., 1970; Garfunkel et al., 1981). It extends from the northern end of the Red Sea divergent plate boundary to the Bitlis convergent plate boundary in southern Turkey (Fig. 1). Along the DST many pull-aparts (e.g. the Dead Sea and Hula basins) and push-ups (e.g. Mount Hermon) developed due to left and right stepovers of the transform trace (Garfunkel, 1981).

Nahal Darga drains the eastern part of the Judean Mountains and the Judean Desert located west of the northwestern part of the Dead Sea pull-apart (Fig. 1). The western margin of the Dead Sea is characterized by a north-south escarpment, about 400–600 m high, comprised of a few topographic steps due to step faulting. This escarpment is subparallel to the DST and is marked as "border faults" of the Dead Sea rift (Fig. 1). It resulted from up to 10 km down faulting due to extension in the vicinity of the Dead Sea (e.g. Kashai and Croker, 1987) that occurred since the Pliocene to the present. Prior to 5 Ma ago the DST was characterized by strike-slip motion (Garfunkel, 1981). However, since then the trend of motion has been changed to an oblique one, as reflected by the change in Euler Pole, and also includes an extensional component along the DST resulting in rift development (Joffe and Garfunkel, 1987). Streams draining the eastern part of the Judean Mountains and Judean Desert into the Dead Sea have incised narrow and very steep gorges, up to a few hundred meters deep, due to the high topographic escarpment. The slope of the riverbeds is steep and many waterfalls developed up to ten kilometers west of the escarpment. The subsidence of the rift block and the depth of the Dead Sea water in this area, about 400 m, created an ideal situation for the development of fan-deltas. The Nahal Darga

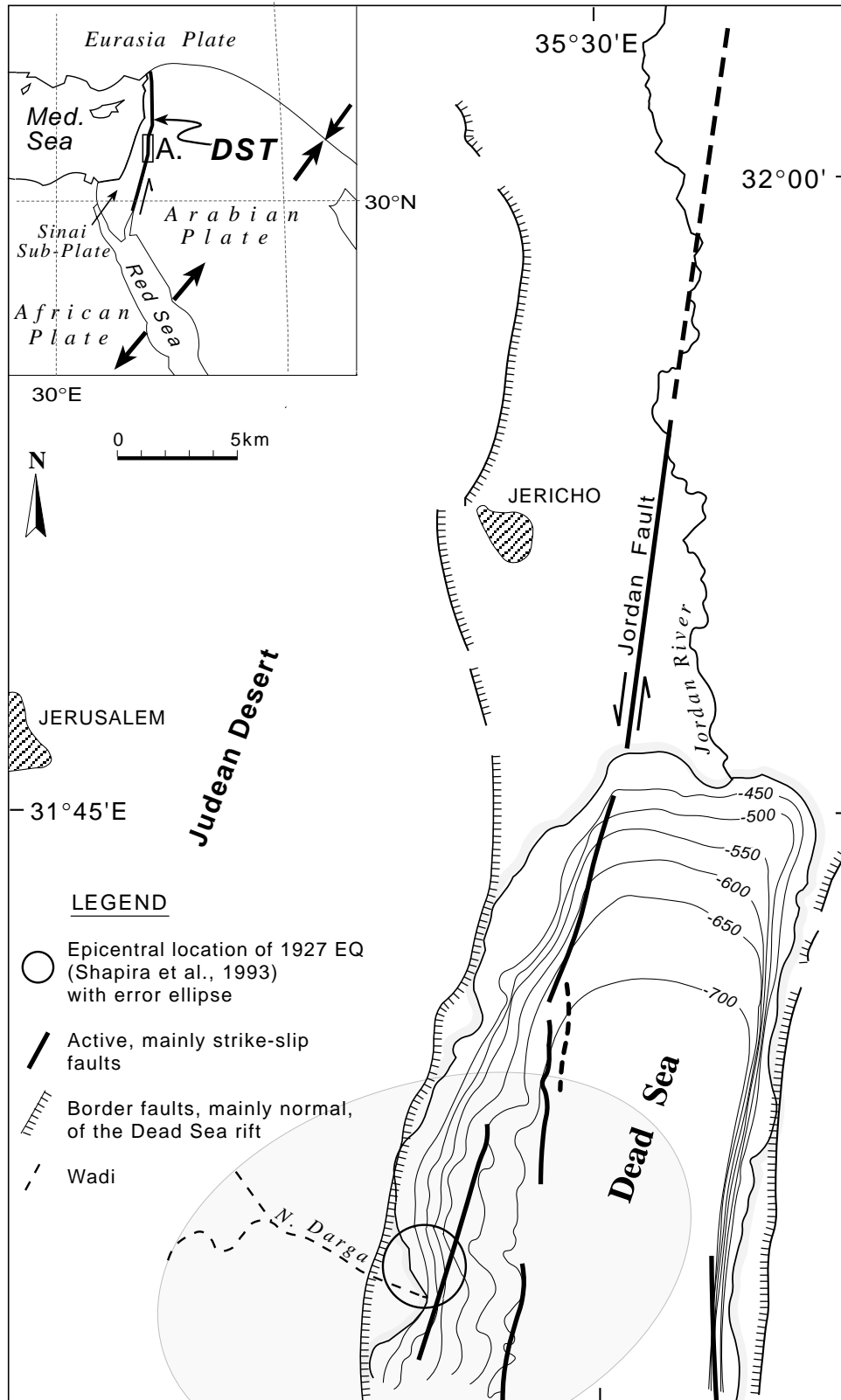


Fig. 1. Location map (after Niemi and Ben-Avraham, 1994) – a general tectonic setting of the Dead Sea transform (A – the study area). Insert – The general tectonic setting of the northern part of the Dead Sea (after Niemi and Ben-Avraham, 1994). The epicentral location of the Jericho 1927 earthquake (Shapira et al., 1993) is about 2 km northeastward of the Nahal Darga fan-delta. The contour lines are the bathymetric contours of the Dead Sea.

fan-delta is the largest in the northwestern part of the Dead Sea.

Fan-deltas are developed in areas where high relief is replaced by low, such as a mountain range front, or margins of deep-water bodies surrounded by high topographic areas. The heavy load carried by the high-energy water, characterizing steep intra-mountain rivers, is deposited as soon as the water loses its potential energy when reaching the lowland. The load is differentially deposited according to the weight of the particles carried, the coarser near the river mouth and the finer away from it.

Commonly, young fan-deltas such as that of Nahal Darga consist of poorly-consolidated or loose sediments. Displacement along exposed fault planes within such fan-deltas is very common (see below) and may result from two mechanisms:

1. landslides triggered by gravitational loading and movement toward the depositional basin, or
2. faulting due to tectonic activity.

It is important to determine which mechanism is responsible for given faults within young deposits, especially for areas with evidence of historical earthquakes such as the Dead Sea, for the following reasons:

1. faults, with different amounts of displacement are common in many fan-deltas which developed within or adjacent to tectonically active areas, e.g. along the DST (Zak and Freund, 1966; Bowman, 1995), in the Basin and Range Province (e.g. Bell and Katzer, 1987), and along the San Andreas Fault (e.g. Sieh and Jahns, 1984); and
2. seismic hazard assessment is frequently based on recurrence time of large earthquakes and this in turn depends on relating the faults and other deformation structures to tectonic events.

The recurrence time of large earthquakes in the Dead Sea area is commonly based on dating of rock units that were displaced along new or reactivated faults (e.g. Reches and Hoexter, 1981; Marco and Agnon, 1995; Enzel et al. 2000). Thus, distinguishing between faults developed due to mass movement toward the basin and faults formed due to tectonic activity is crucial in an attempt to assess the seismic risk and recurrence time. The existence of deep-seated subsurface faults beneath a group of exposed faults in a fan-delta would strongly support the development of the latter due to tectonic activity, whereas the lack of such faults or the existence of a shallow detachment surface may support a landslide mechanism (e.g. Hoek and Bray, 1991).

In this paper we report the results of a geologic and seismic study in Nahal Darga fan-delta. It shows the association between surface faults and underlying subsurface faults precisely identified by detailed field mapping and a high-resolution seismic survey. This association suggests that the Holocene fan-delta surface faults are the extension of deep-seated larger faults.

2 Geological geomorphological setting

The Dead Sea transform, together with the North Anatolian and South Anatolian faults, is one of the main tectonically active zones in the Middle East responsible for large and hazardous earthquakes (e.g. 1927 Jericho earthquake, and 1999 Izmit earthquake along the DST and North Anatolian Fault respectively). The pre-Holocene history of the tectonic activity along the DST is based mainly on the analysis of displaced rock units along faults associated with this activity (e.g. Freund, 1965; Freund et al., 1970; Bartov, 1974; Garfunkel, 1981; Eyal et al., 1981), as well as other deformation structures, such as folds and pull-aparts or pushups. The latter resulted from the en-echelon and stepover patterns of the DST trace (Ben-Avraham, 1985; Freund, 1965; Garfunkel, 1981; Heimann and Ron, 1987; Eyal et al., 1981). The Late Pleistocene to Recent history of seismic activity has been based on a variety of features, e.g. faults within Late Pleistocene and Holocene terraces (e.g. Bowman and Gerson, 1986; Gardosh et al., 1990; Enzel et al., 2000); slumps in the Jordan River sediments (Niemi and Ben-Avraham, 1994); analysis of deformed young sediments within trenches excavated across active faults (Reches and Hoexter, 1981; Amit et al., 1997); fluidized beds associated with surface faulting such as those found in the Lisan formation (Marco and Agnon, 1995); liquefaction structures (Enzel et al., 2000), destruction of archeological sites (e.g. Karcz et al., 1977; Ben-Menahem, 1991; Marco, et al., 1997), and monitored displacement of key blocks due to seismic activity (Hatzor, 1999).

Faulted scarps in Holocene rocks along the DST are abundant and were reported from various locations along the DST, for example: at the northwestern margin of the Gulf of Elat (Bowman and Gerson, 1986); within the municipal area of the city of Elat (Ginat et al., 1994); the southern Arava north of Elat (e.g. Zak and Freund, 1966; Gerson and Grossman, 1991; Enzel et al., 1994); the Dead Sea area (e.g. Gardosh et al., 1990; Cadan, et al., 1996; Bowman, 1995); and the Hula Basin in northern Israel (Heimann et al., 1997).

Nahal Darga, as one of a number of streams draining the Judean Mountains and Judean Desert, crosses the fault escarpment of the Dead Sea rift into the northwestern part of the Dead Sea basin. It terminates in an active fan-delta comprising of poorly consolidated, Late Pleistocene and Holocene, fluvial, deltaic and lacustrine sediments (Enzel et al., 2000). The eastern part of the Nahal Darga fan-delta (Fig. 1) is close to, or even overlaps, the southern extension of the Jordan Fault that is one of the active segments of the DST (Niemi and Ben-Avraham, 1994). The mouth of this fan-delta is located about 2 km from the revised location of the epicenter of the 11 July 1927, M_s 5.9, Jericho earthquake which supposedly occurred due to the reactivation of this fault (Shapira et al., 1993). The maximal distance from the Nahal Darga fan-delta to this epicenter will not exceed 12 km even if it occurred at the farthest point from the fan-delta but within the error ellipse. This implies that a considerable part of the deformation in this area should be associated

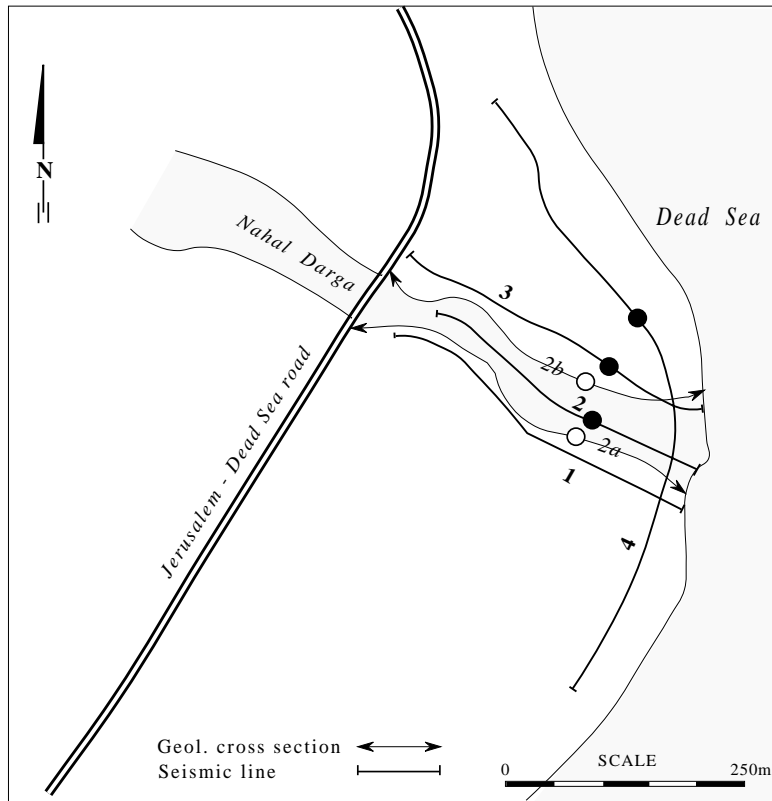


Fig. 2. The Nahal Darga fan-delta and its incised channel, the shaded area between (2a) and (2b). The outline of the seismic profiles is in heavy lines, and the numbers 1 to 4 represent the seismic profile lines 1 to 4. The southern geologic cross section of the channel walls, (a), and the northern one, (b), are outlined by thin line with arrows. The open circles on the channel walls represent the location of the exposed allochthonous bodies and the highly deformed blocks in the southern and northern channel walls respectively. The full circles on the seismic profiles represent the first appearance, from west, of the large subsurface reverse faults and flower structures representing the western boundary of the eastern deformation zone (S.P. 100, 140 and 190 in profiles 2, and 3, and 4, respectively).

with seismic activity.

The Dead Sea lake level underwent significant changes during the late Pleistocene and Holocene (e.g. Bowman, 1971; Neev and Hall, 1977; Klein, 1982; and Frumkin et al., 1994). During the last 30 years the Dead Sea lake level was lowered at a mean rate of about 70 cm per year. This lowering, by more than 20 m (Klein, 1982), is the consequence of human intervention by using the sweet water of the Dead Sea drainage system for human need. Due to this change in the Dead Sea lake level, the easternmost part of the fan-delta (Fig. 2) was incised by a 7–10 m deep channel exposing the Late Pleistocene and Holocene section. A geological and structural study, including detailed mapping of the channel walls that was performed by Kadan (1997) is the basis of the geological part of this study. It reveals the detailed structure of the fan-delta and the relationship between its gently east dipping (up to 5° – 7°) sedimentary units composed of conglomerates, sandstones, silts and clays (Fig. 3, (Cadan et al., 1996; Enzel et al., 2000)). The conglomerates represent deposition along the riverbed, or even within the lake in cases of floods. Very low dips of the conglomerate cross-sets characterize deposition along the riverbed, whereas high dips, up to a few tens of degrees (e.g. Fig. 3a, 370, unit 12), charac-

terize deposition in the lake depending on the water depth. The sandstones represent deposition along a beach environment, and the silt and clays were deposited within the water lake. Due to the frequent changes of the Dead Sea lake level during the Pleistocene and Holocene, the deposition location of each type of sedimentary unit changed in space. During lake high stands sediments such as clays, carbonates and silts, were deposited west of the present shoreline (e.g. Fig. 3a, unit 7, 115–160) because the lake extended westward. On the other hand during low stands, the deposition location of deltaic sandy gravely sediments was shifted to the east (e.g. Fig. 3a, unit 12, 360–420) due to the eastward retreat of the lake. In addition, field relationships indicate that during lake level lowering major erosional unconformities (e.g. Fig. 3b, 0–100; Fig. 3a, 140–200) were developed. At the eastern part of the fan-delta the regular, gently dipping cross-bedding sets change to very steep foresets of coarse grained deposits (Gilbert Type sets (Fig. 3a, unit 12, 360–415), commonly characterizing deposition on steep slopes (Massari and Colella, 1988).

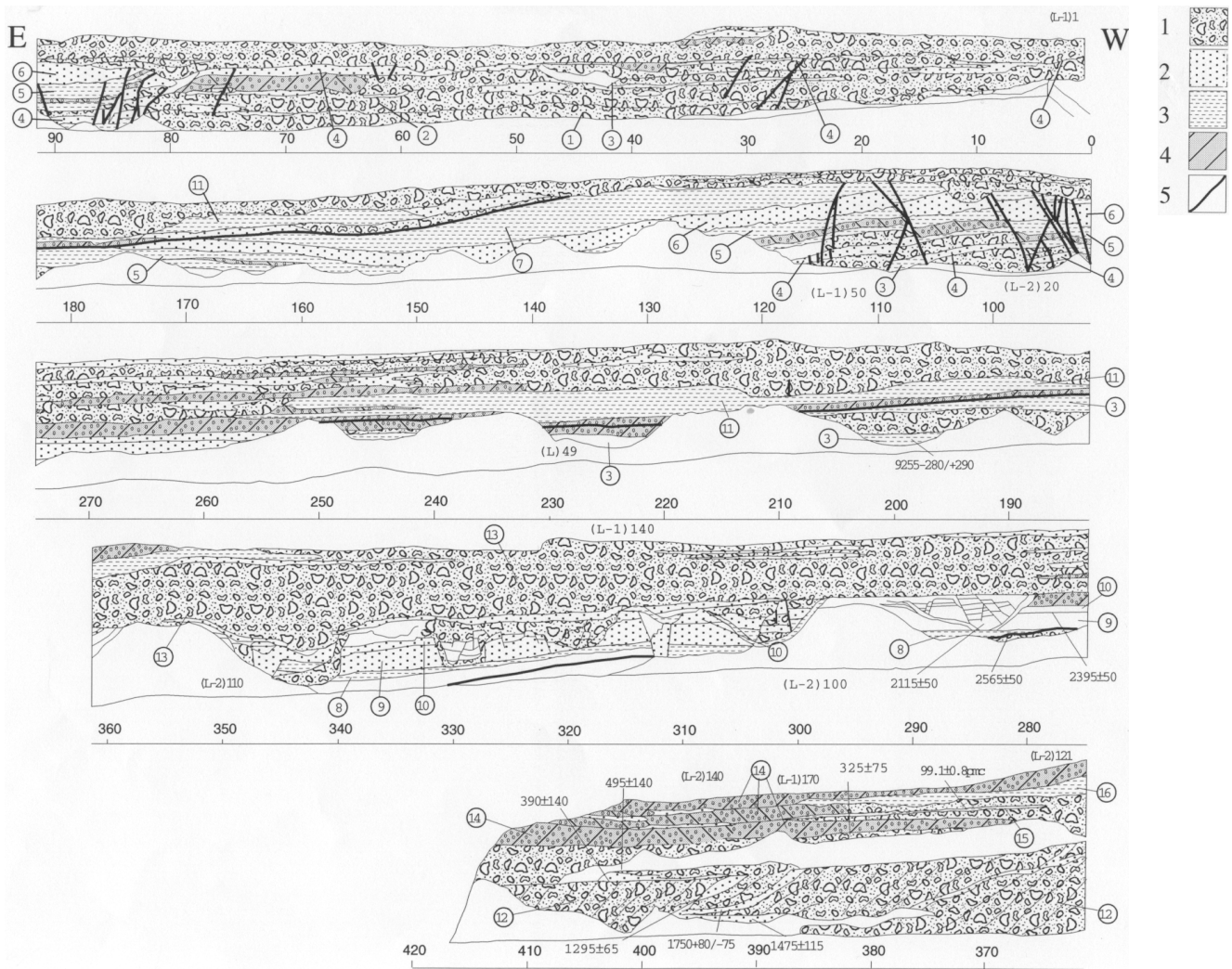


Fig. 3a. A continuous stratigraphic cross section along both channel walls of Nahal Darga fan-delta and Shot Point of the seismic profiles. Figure 3a presents the southern wall and 2b the northern one. The left end of each section of Fig. 3a is continued with the right end of the section below it, and the right end of each section of Fig. 3b is continued with the left end of the section below it. The lower scale is in meters; Numbers in circles represent stratigraphic units from the older to the younger ones, and the heavy line is the major unconformity crossing the study area. Important shot-points, drawn above or below the cross-section, represent the location of subsurface faults beneath the stratigraphic cross section. The number of profile line appears in brackets and the shot-point beside it.

The legend: 1. conglomerate; 2. Sandstone; 3. silt and shales; 4. cross-bedding; and 5. fault line. These stratigraphic cross sections are based on tracing the main rock units on scaled photographs.

3 Faults and deformation zones in the Nahal Darga fan-delta

A full description of the various rock units comprising the stratigraphic section and the deformation features is found elsewhere (Enzel et al., 2000). In this section we briefly describe the structures that are relevant in examining the possible association between the surface and subsurface structures. The precise determination of surface faulting, even to a scale of a few centimeters, is facilitated by the various types of sediments with sharp bedding planes comprising the fan-delta and the intervening distinct unconformity planes (Fig. 3). A detailed structural study reveals the exist-

tence of two deformation zones. The most dominant structures in the western zone are two sets of faults (Fig. 3a, 75–115) whose mean strike is NNE-SSW and a mean dip 60° – 70° to WNW or ESE (Fig. 4). The displacement along these faults varies from a few centimeters to 2 m. A few faults crosscut almost the entire section (e.g. Fig. 3b, 30), whereas the majority are either covered by continuous unfaulted beds (e.g. Fig. 3a, 80–100), or affect only a few beds (e.g. Fig. 3b, 275–285). Along some of the faults multiple faulting could be proved according to differential displacements along their fault planes in which the displacement of the lower beds is consistently higher than those of the upper strata (Enzel et

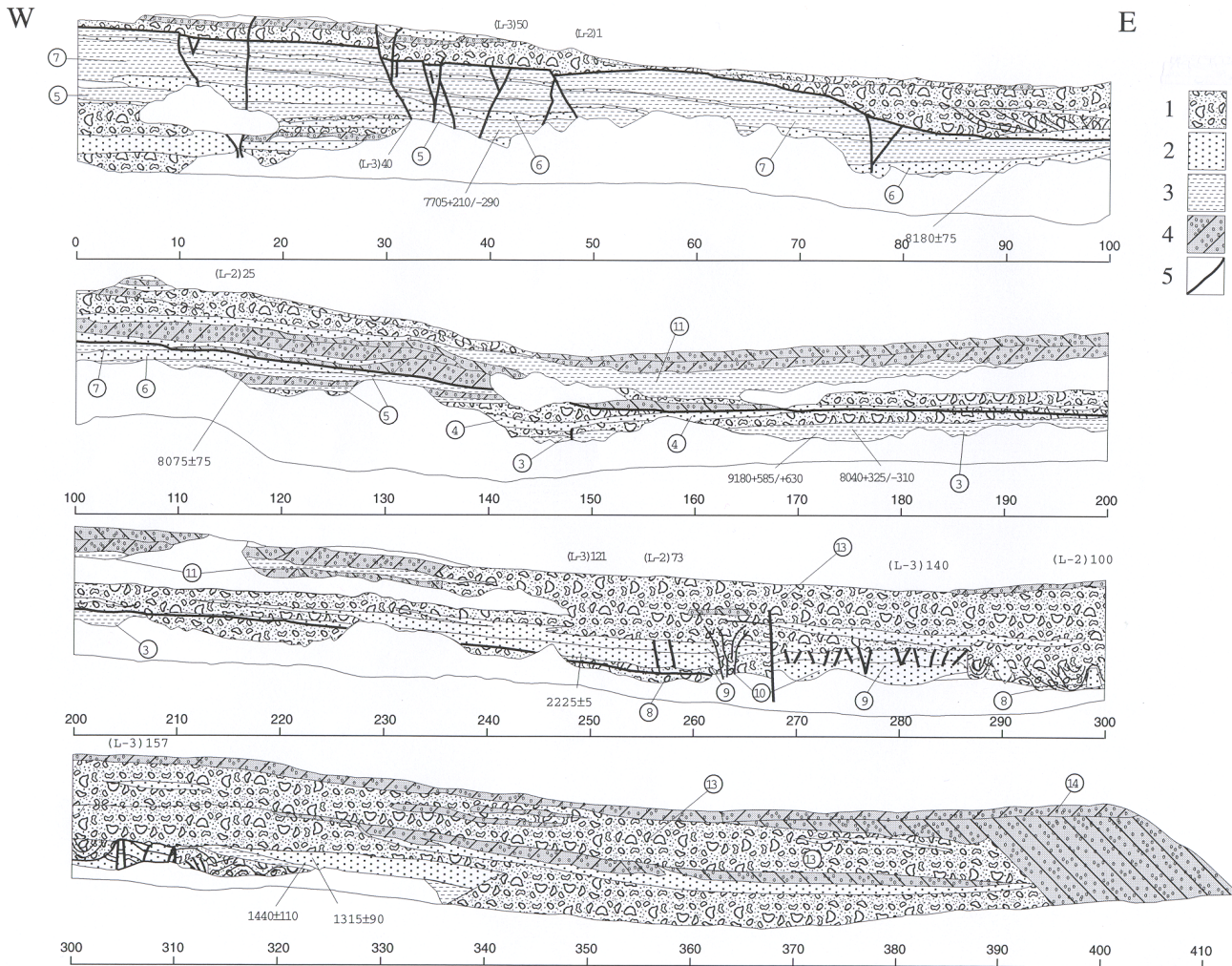


Fig. 3b. continued ...

al., 2000). Assuming that the faulting resulted from tectonic activity, such multiple displacements indicate reactivation of the faults due to a few sequential earthquakes that occurred at different times during the deposition of the fan-delta (Cadan et al., 1996). The faults in the eastern deformation zone are short and cross only a few layers (e.g. Fig 3b, 255–285). The eastern deformation zone is also characterized by a different deformation style. Three rock bodies, about 15 m wide, and a bowl-shape cross-section are exposed along the southern wall of the channel (Fig. 3a, 280–290, 300–307 and 327–331). A few layers including rotated and faulted blocks up to a few meters long and high (Fig. 3b, 287–320) are exposed in the northern wall, NNE of the bowl-shape bodies only there. These bodies, on both sides of the channel, are restricted to one horizontal stratigraphic zone up to 5 m thick and are located above a continuous silty layer (unit 8, Fig. 3a) with no deformed beds above or below. Internal faults and deformation features such as mixed layers (Marco and Agnon, 1995) were observed in the rocks comprising the bowl-shape bodies but not in the adjacent rock of the fan-delta. Enzel et al. (2000) suggested that these allochthonous bodies are

most probably slumps and represent another style of deformation caused by medium to large earthquakes. However, the NNE-SSW trend, including the allochthonous bodies and the rotated blocks, is parallel to the mean strike of all faults in the fan-delta, and is located above sub-surface faults.

At least ten layers containing liquefaction structures were observed in the fan-delta within the fine-grained sandy and silty lacustrine sediments. The scatter of the liquefied layers in the stratigraphic section is uneven, several groups of adjacent layers underwent liquefaction, whereas other groups with similar composition but at different levels of the section, did not undergo such liquefaction. These liquefaction structures indicate continuous seismic activity in this area. The groups of closely overlying liquefied layers indicate a cluster of large earthquakes whereas the unliquefied groups indicate quite period. Radiocarbon dating of part of the liquefied strata suggests a mean recurrence frequency of approximately 600 years for magnitude >5.5 earthquakes (Cadan et al., 1996; Enzel et al., 2000). However, the faults within the two deformation zones could result from either displacements due to deep-seated faults or from gravitational slump-

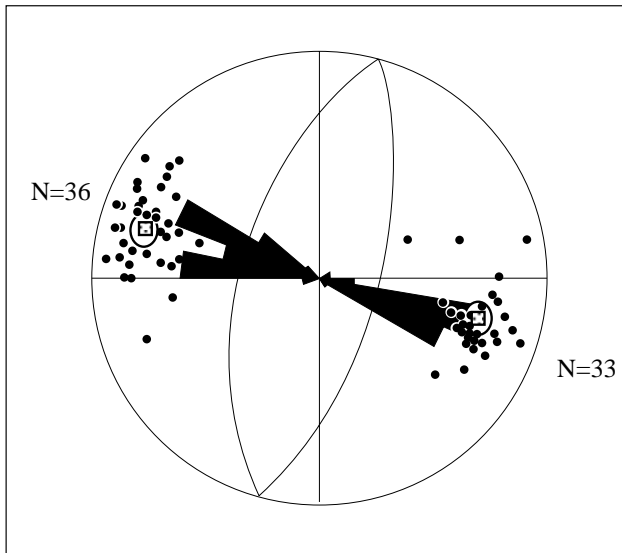


Fig. 4b. Stereographic projection, lower hemisphere, of 99 poles (dots) to fault planes from Nahal Darga. The great circles are the mean fault planes of the two groups of faults striking NNE-SSW with dips to WNW and ESE. The small circles outline the $\alpha 95$ range.

ing (Selby, 1982) of the sedimentary sequence as a response to the existence of a deep basin to the east.

4 Shallow high resolution seismic study

4.1 Data acquisition

High-resolution seismic profiles were acquired in order to study the subsurface in the Nahal Darga fan-delta. Profiles 1, 2, and 3 (Figs. 5a, 5b, 5c, respectively) were located along the southern bank, the stream channel and the northern bank, respectively (Fig. 2). Profile 4 (Fig. 5d) is arcuate because it follows the Dead Sea coastline. The data acquisition system consisted of an EG&G recording system. The seismic source was a Dynasource pneumatic hammer hitting the ground, two shots per location, and the seismic line comprised 10 Hz geophones and an off-end cable spread consisting of 48 channels with minimum offset of 5 m and 2.5 m between receivers. The maximum common depth point (CDP) fold was 12 traces and source interval was 5 m. The total recording time was 1 s. with a sample rate of 0.0005 s.

4.2 Data processing

The processing sequence for all CDP stacked data was similar to conventional petroleum exploration processing flows, with the main distinctions related to scale and emphasis on event identification after each processing step. Note that the term “high resolution” is not only the recording parameters, but also the processing scheme of the recorded data; thus special attention during the processing step was paid to mute

determination. In particular, it is well known (Miller, 1992) that selection of improper normal moveout (NMO) mute on shallow reflection data can drastically degrade the quality of CDP stacked sections. Stacking velocities were determined through qualitative analysis of constant velocity stacks and were followed by post-stack time migration.

Prestack depth migration would have been more appropriate in this study but it requires an accurate and detailed knowledge of the shallow subsurface. Because of the lack of this information we did not use this process.

5 Results

We represent here only the results of the reflection wave profiles, although exact determination of fault location within the profile is also based on diffraction waves. Usually the detection of faults on seismic sections is solved by visual interpretation of stacked sections. However, when detecting faults with a vertical displacement of less than the wavelength, a more sophisticated method must be used. In order to obtain reliable information about possible structural/lithological discontinuities from seismic data, a procedure utilizing certain features known to be associated with the presence of such discontinuities is desirable. One such specific feature demonstrating the presence of faults on a seismic section is associated with the presence of diffracted waves in the vicinity of the discontinuity location. These waves can serve as a good indicator for fault detection. We extracted diffractions from the unmigrated stacked sections and used this information for identifying real discontinuities in the subsurface. A detailed description of the method and examples of its application may be found in Landa et al. (1987) and Bruner and Landa (1991).

The seismic interpretation is based on the presence of reflection horizons which, most probably but not necessarily, imply stratigraphic correlation. The time is given in seconds by Two Way Time (TWT). Based on a priori information (Niemi and Ben-Avraham, 1997; Ben-Avraham, 1997; Kashai and Croker, 1987), average velocity in the investigated area is about 2000–2500 m/s, so the maximal information depth achieved by these seismic profiles is about 400 m. **Profile 1** (GI-047-EG; Fig. 5a): This profile is disturbed in its central part, (Shot Points (S.P.) 55–135) due to its proximity to the steep southern wall of the stream channel (Fig. 2). Nevertheless, in its western part (S.P. 30–55) the subsurface bedding dips gently eastward and one normal fault can be determined. This fault is located below the eastern part of the western deformation zone (Fig. 3a, 115). At the eastern part of this profile (S.P. 137–150) two normal faults are defined below the area in which the allochthonous bodies are exposed at the surface (Fig. 3a, 315).

Profile 2

(GI-048-EG; Fig. 5b): This profile was measured in the middle of the Nahal Darga channel and, therefore, can be related to both channel walls. The western termination of this seismic line lies approximately at the eastern part of the west-

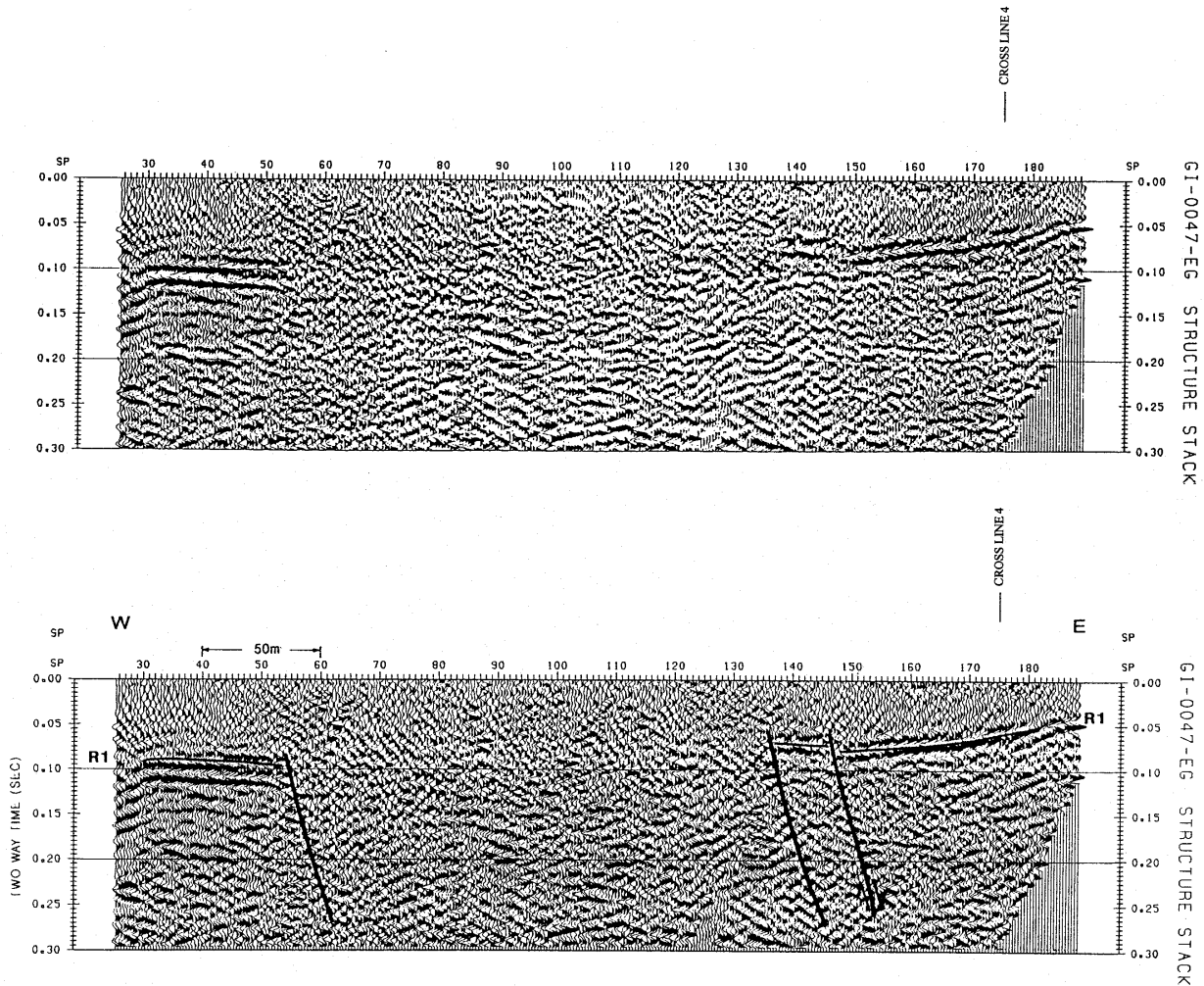


Fig. 5a. Uninterpreted and interpreted multichannel high-resolution seismic profiles from the Nahal Darga fan-delta. The location of these profiles is found in Fig. 2. The interpreted seismic markers do not have any stratigraphic correlation. The exact determination of fault location within the profile is also based on diffraction waves. The time is given in seconds by Two Way Time (TWT). The vertical lines above the seismic profiles in each of the profiles relate to the crossing location of seismic profiles. For example, the vertical line at the eastern part of profile 1 is the location where profile 4 crosses profile 1. The three vertical lines above profile 4 are the locations where, from left to right, profiles 3, 2 and 1 cross profile 1 respectively.

ern deformation zone. No overlap exists between these two because an artificial waterfall, designed to protect the road where it crosses the riverbed, prevented installation of the geophysical equipment further to the west. Therefore, the faults of the western deformation zone could not be detected in this seismic profile. The subsurface bedding dips gently toward the east as expected of fan-delta layers which drain eastwards. An overall subsurface positive flower structure, comprised of a major reverse fault associated with a cluster of minor normal faults and a gentle fold, is outstanding between S.P. 100–130 and 0.05 s TWT. The location of these subsurface faults is below the area of the allochthonous bodies in the southern channel wall (Fig. 3a, 300) and the deformed blocks in the northern wall (Fig. 3b, 300). At S.P. 140 a normal fault is observed in the subsurface extending almost to the surface. This fault is located east of the eastern defor-

mation zone and underneath the surface area in which the bedding and cross-bedding become steep, Gilbert type sets (Fig. 3a, 395). Development of steeply dipping cross sets is commonly associated with deposition in deep water and, therefore, the existence of deep-seated normal faults beneath these sets may suggest deepening of the lake near the coast due to down faulting. At S.P. 65–80 and 0.06–0.1 s (TWT) a concave unconformity, probably the trace of an old small channel, is observed. This is similar to small erosional channels within the surface section (e.g. Fig. 3a, 102, upper part of the section) or to the surface slumps.

Profile 3

(GI-049-EG; Fig. 5c): This profile is characterized by intensive normal faulting, which at S.P. 45–80 forms a flower structure pattern with a gentle fold between the secondary faults at S.P. 80, 0.1 s TWT. The main subsurface fault, at

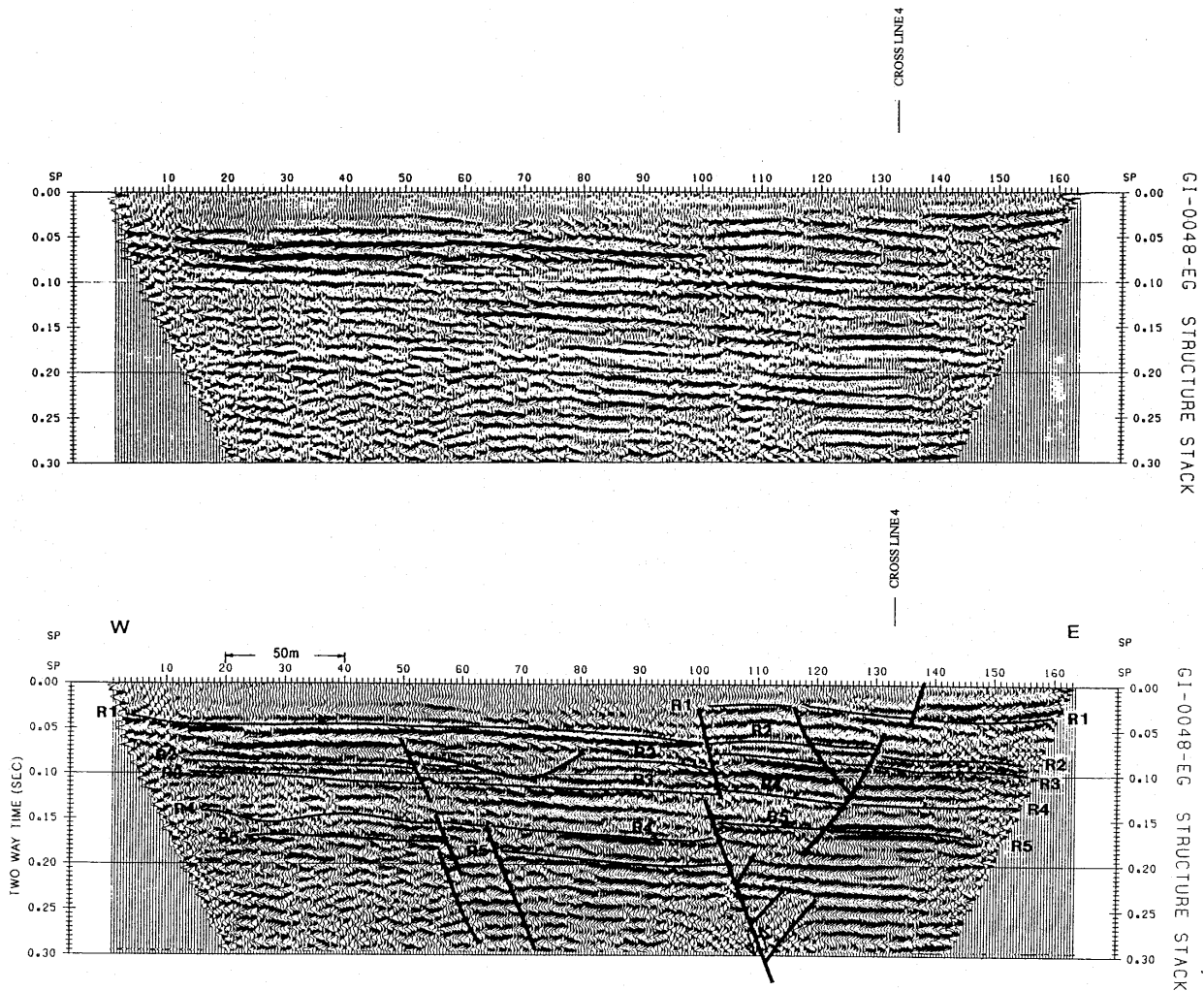


Fig. 5b. continued ...

S.P. 50, overlaps the intensively faulted area of the western deformation zone along the northern channel wall (Fig. 3b, 30–50). Actually, this subsurface fault is found along the continuation of a surface fault that exhibits the largest observed vertical displacement in this fan-delta. At the eastern part of the profile a large reverse fault (its upper part at S.P. 138, and lower at 157) which forms the western boundary of a gentle anticline (its hinge at S.P. 160 and 0.07 s TWT) is observed. This reverse fault is located just below the eastern deformation zone in the northern bank of the channel (Fig. 3b, 275–314). Thickening and thinning of sedimentary layers and a small erosional channel are seen at S.P. 140–200, 0.05–0.15 s (TWT). A 25 m wide, bowl shaped unconformity is observed at S.P. 170 and 0.1 s (TWT) representing either an old buried channel or an allochthonous body.

Profile 4

(GI-050-EG; Fig. 5d): This profile, measured along the Dead Sea coast, includes three different domains. Flat bedding, and a few normal faults characterize the southern domain, up to S.P. 70. In the second domain (S.P. 70–190) the general subsurface pattern is that of a positive flower structure in which the strata are intensively deformed by many normal and a few reverse faults and folds between the faults. The third domain (S.P. 195–305) is characterized by continuous bedding gently dipping southeastward. At S.P. 255 and time 0.1 s (TWT) the strata are discontinuous and the bowl shape of the discontinuity is similar to the cross section of the exposed allochthonous bodies in the eastern deformation zone (e.g. Fig. 3a, 285 and 303 lower part), or an erosional channel. This similarity suggests a common mechanism of development for the surface and subsurface stream erosion or allochthonous bodies. An unconformity including stratigraphic reduction of the thickness between two markers is observed between S.P. 190–300 and time 0.1–0.12 s (TWT). There is a general consistency between the structures around the intersection points of line 4 with lines 1, 2, and 3.

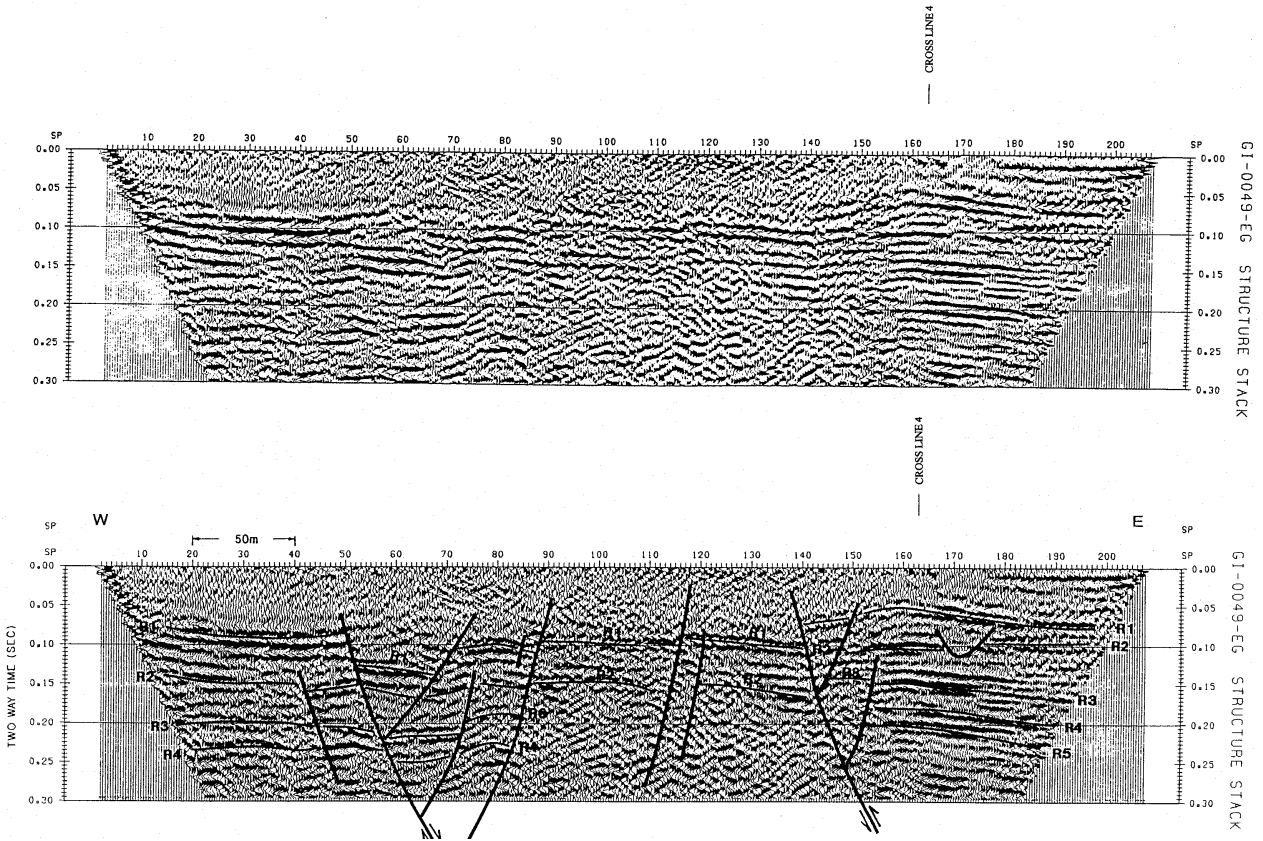


Fig. 5c. continued ...

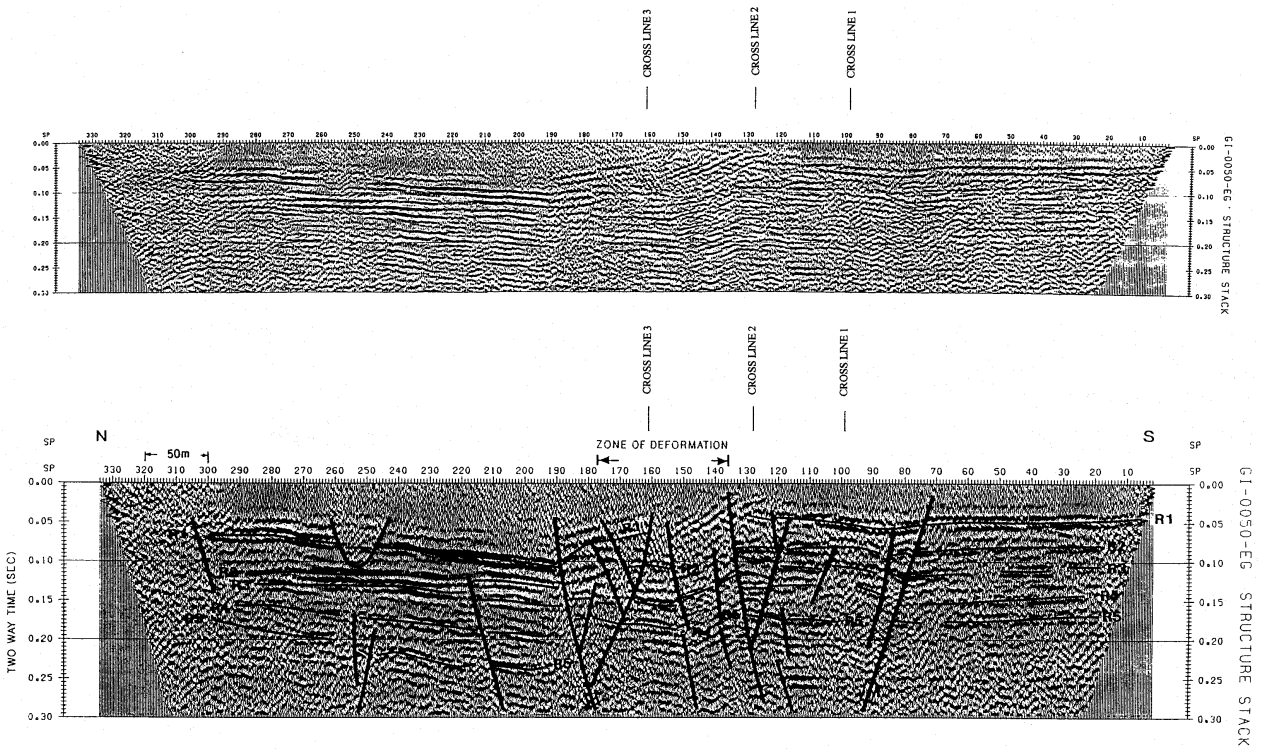


Fig. 5d. continued ...

6 Discussion

Due to the constraints of shallow high-resolution seismic data acquisition, reliable seismic data begin at a depth of approximately 10 m and extend to about 400 m. This range of seismic information results in a +10 m zone, immediately below the surface, that lacks both surface geological information and seismic data. However, the proximity of the surface data to the subsurface data justifies the correlation between the two. The interpreted stacked sections of profiles 1–3 (GI-047-EG, GI-048-EG, and GI-049-EG respectively) reveal a general eastward dip as expected of a fan-delta draining eastward. In profile 4 (GI-050-EG), the dips are subhorizontal in the southern part and have a SE component in the northern part. These dips are expected from the NE trend of the southern part of this profile that is perpendicular to the trend of Nahal Darga and the NW trend of the northern part of profile 4 that is oblique to the Nahal Darga stream. Similar dip-trends are seen, as expected, in the northern, eastern, and southern parts of the other fan-delta in this region. In addition to the similarity of surface and subsurface dips other geomorphologic features characteristic to fan-deltas, such as thinning and thickening of sediment layers and cut and fill small channels filled with younger sediments, are also observed. These observations indicate that the depositional conditions that prevailed in the fan-delta area during the Holocene also existed in earlier times, while the subsurface sediments, to the depth of 400 m, were deposited.

The main seismic reflectors determined in the profiles should be bedding or unconformity planes as no other planes were observed in the fan-delta exposed section. These reflectors are displaced along discrete planes, faults, similar to the displacements of the surface bedding, indicating that faulting is not limited to the upper part of the fan-delta but extends down to at least the Late-Pleistocene subsurface rock units.

It could be argued that displacements along the fault planes in the fan-delta section resulted from movements due to tension cracks in the upper block of a landslide. Such landslides could develop either as plane failure along dipping clay beds (e.g. Selby, 1982; Hoek and Bray, 1991) or as slumps along shallow, spoon-shape, sliding planes (circular failure, Hoek and Bray, 1991), without any direct association to subsurface faults. The internal friction angle of soft sedimentary rocks such as sandstone, chalk and shale is in the range of 25°–35° (Hoek and Bray, 1991, Table 1). A smaller friction angle, 16°, was measured by Hatzor and Levin (1997) for clay filled bedding plane in limestones along which a plane failure occurred in a phosphate mine. However, the development of the faults within the Nahal Darga fan-delta due to landslides is rejected because:

1. no shallow curved planes, along which slumping could occur, were detected in the seismic profiles to the depth of 400 m, and
2. the gentle dip of the bedding comprising the fan-delta, 3°–7°, is too shallow to initiate sliding toward the lake.

A tectonic origin, most probably associated with seismic activity along the DST faults, is suggested as the cause of the various structures developed in the fan-delta for the following reasons:

1. subsurface faults, displacing the reflectors in the buried section, extend from a depth of at least 400 m, which is the depth of the seismic resolution, almost to the surface;
2. the good correlation observed in many cases between surface and subsurface faults suggests association between them. A good example is the continuation between the subsurface fault observed in the western part of profile 3 (with the reservation of the upper 10 m gap between the surface and subsurface data) with the surface fault along which the largest vertical displacement in this fan-delta was measured; and
3. the low inclination of available sliding planes (3°–7°) with respect to the available friction angle between the layers (16°–25°).

Along several subsurface faults the displacement is limited to the subsurface and does not continue upwards (e.g. profile 4, S.P. 220 and profile 3, S.P. 40). Such buried faults indicate old faults that were not reactivated by younger tectonic events, similar to many surface faults, (e.g. Fig. 3a, 78–86). The thinning of layers toward the flower structure in profile 5d, S.P. 300–190, is best explained by a small high at S.P. 190, formed most probably due to faulting. This implies that the faulting and flower structure development has been active since the deposition of Nahal Darga section during the Pleistocene.

The correlation between surface and subsurface faults is also suggested by the different deformation style characterizing the two surface deformation zones and their concurrence in the subsurface. The surface western deformation zone of the fan-delta is characterized by NNE trending normal faults whereas that of the eastern zone is different and includes only small faults confined to three layers (northern cross section, Fig. 3b, 268–285) and highly deformed strata (Fig. 3b, 280–320) and three NNE trending allochthonous bodies (slumps) (Fig. 3a, 280–350). The surface NNE trend of these allochthonous bodies is suggested by correlating them with the highly deformed strata in the northern wall. The first appearance of the allochthonous bodies and the highly deformed strata in the cross sections (Figs. 3a, 3b) is denoted by empty circles on cross sections 3a and 3b (Fig. 3), respectively. This NNE trend is parallel with the mean strike of the small faults in this area (Fig. 4). The deformation style of the fan-delta subsurface also depends on the location along the fan-delta. The subsurface faults in the western part of the fan-delta are mainly normal (e.g. Fig. 5c, S.P. 50), whereas the seismic reflectors in the eastern part include evidence of both normal and reverse faults in a positive flower structure pattern suggesting some compression along this zone.

The true strike of the subsurface faults is unknown, however it could be estimated by comparing the trends of deformation zone boundaries at surface and subsurface. The first appearance, from the west, of the large subsurface reverse faults and flower structures representing the western boundary of the eastern deformation zone (S.P. 100, 140 and 190 in profiles 2, and 3, and 4 respectively) were marked on Fig. 2 as full circles. The general trend of these circles, and hence the trend of this boundary, is NNE and it is parallel with:

1. the mean strike of the exposed surface faults in the fan-delta (Fig. 4);
2. the line connecting the first appearance of the allochthonous bodies in the southern wall and the highly deformed strata in the northern wall.

From Fig. 2 it is clear that the line of first appearance of the allochthonous bodies in the southern wall and the highly deformed strata in the northern wall are very close to the line of first appearance of the large reverse faults and flower structures in the subsurface. This association strongly supports correlation between them. The existence of a positive flower structure fault pattern comprised of normal and reverse faults and secondary folds (Twiss and Moores, 1992) in the subsurface of the eastern deformation zone suggests tectonic activity under a compressional component, although most surface faults are normal. These relationships may be explained by assuming N-S left-lateral movement along the NNE trending eastern deformation zone. Such a left-lateral movement should be attributed to tectonic activity along the Jordan fault (Fig. 1), or to one of its secondary splays that extends under the eastern deformation zone of the fan-delta, or very close to it. The compressional nature of the subsurface faulting in the eastern part of the fan-delta also explains the difference between the nature of the western and eastern surface deformation zones observed in the fan-delta.

7 Conclusions

Using the Nahal Darga fan-delta case study we show how the combination of a detailed geological mapping and a shallow, high-resolution reflection study reveals the association between surface deformation and subsurface faulting. This association is based on the co-existence of surface deformation zones and subsurface major faults beneath them. These relationships exclude the possibility that the faults in the fan-delta resulted from incipient landsliding. The similarity of surface dips in different parts of the fan-delta and the geometry of the exposed unconformity planes and channels with their counterparts in the subsurface, suggest that Holocene sedimentation actually started in Late Pleistocene. The surface and subsurface deformation styles in the western deformation zone are different from that in the eastern one. The subsurface normal displacements below the western deformation zone and the positive flower structures in the subsurface of the eastern one are in agreement with the sur-

face structures, normal faults in the west and tectonic allochthonous bodies (slumps) due to strike-slip movement in the east. Thinning and thickening of sub-surface strata associated with fault and flower structures suggest that faulting was already active during the Late Pleistocene. The presence of a fault zone underneath the Gilbert Type (steep dipping, up to 20°–30°) sets suggests that the relatively deep water in which the steep sets were deposited probably resulted from near shore faulting.

It is suggested that high-resolution seismic data may be used in other tectonically active localities to distinguish between faulting associated with gravitational mass movement (slumping, land slides and plane failures), and faulting due to tectonics. Such an analysis and interpretation of cross sections is essential in any attempt to calculate the recurrence time of large earthquakes.

Acknowledgements. This study was supported by the Ministry for Energy and Infrastructure. We are grateful to Prof. M. Gross, Dr. Y. Hatzor, Dr. Ch. Benjamini, Prof. A. Ginzburg, Ms. D. Artzi, and an anonymous reviewer for their critical reviews of this paper.

References

- Amit, R., Zilberman, E., Porat, N., and Enzel, Y.: Geomorphic and paleoseismic evidence for large historical earthquake in the Avrona Playa – Dead Sea rift, *Geol. Soc. Isr. Annual Meeting, Kefar Gila'di*, 3, 1997.
- Bartov, J.: A structural and paleogeographical study of the central Sinai faults and domes, Ph.D. Thesis, Hebrew Univ. Jerusalem, 143p (in Hebrew, English abstr.), 1974.
- Bell, W. B. and Katzer, T.: Surficial geology, hydrology, and late Quaternary tectonics of the IXL Canyon area, Nevada. As related to the 1954 Dixie Valley earthquake, *Nevada Bureau of Mines and Geology, Bull.* 102, 52p, 1987.
- Ben-Avraham, Z.: Structural framework of the Gulf of Elat (Aqaba), northern Red Sea, *J. Geophys. Res.*, 90, 703–726, 1985.
- Ben-Avraham, Z.: Geophysical framework of the Dead Sea: Structure and Tectonics; *The Dead Sea, Oxford Monographs on Geol. and Geophys.*, 36, 22–35, 1997.
- Ben-Menahem, A.: Four thousands years of seismicity along the Dead Sea Rift, *J. Geophys. Res.* 96(B12), 20 195–20 216, 1991.
- Ben-Menahem, A., Nur, A., and Vered, M.: Tectonics, seismicity and structure of the Afro-Eurasian junction – The breaking of an incoherent plate, *Phys. Earth Planet. Inter.*, 12, 1–50, 1976.
- Bowman, D.: Geomorphology of the shore terraces of the Late Pleistocene Lisan Lake, Israel, *Paleoeco. Paleoclim. Paleoecol.*, 9, 183–209, 1971.
- Bowman, D.: Active surface ruptures on the northern Arava fault, the Dead Sea Rift, *Isr. J. Earth Sci.*, 44, 51–52, 1995.
- Bowman, D. and Gerson, R.: Morphology of the latest Quaternary surface faulting in the Gulf of Elat region, eastern Sinai, *Tectonophysics*, 128, 97–119, 1986.
- Bruner, I. and Landa, E.: Fault interpretation from high resolution seismic data in the northern Negev, Israel, *Geophysics*, 56, 7, 1064–1070, 1991.
- Cadan, G., Bruner, I., Eyal, Y., Enzel, Y., and Landa, E.: Correlation between surface and subsurface structures at the Holocene fan-delta of Nahal Darga, Dead Sea, *Geol. Soc. Isr. Annual Meeting, Elat*, p. 16, 1996.

- Enzel, Y., Amit, R., Bruce, J., Harrison, J., and Porat, N.: Morphologic dating of fault scarps and terrace risers in the southern Arava, Israel: Comparison to other age-dating techniques and implications for paleoseismicity, *Isr. J. Earth Sci.*, 43, 91–103, 1994.
- Enzel, Y., Kadan, G., and Eyal, Y.: Holocene Earthquakes in the Dead Sea Graben from a Fan-Delta Sequence, *Quaternary Research*, 53, 34–48, 2000.
- Eyal, M., Eyal, Y., Bartov, Y., and Steinitz, G.: The tectonic development of the western margin of the Gulf of Elat (Aqaba) Rift, *Tectonophysics*, 80, 39–66, 1981.
- Freund, R.: A model of the structural development of Israel and adjacent areas since Upper Cretaceous times, *Geol. Mag.*, 102, 189–205, 1965.
- Freund, R., Garfunkel, Z., Zak, I., Goldberg, M., Weissbrod, T., and Derin, B.: The shear along the Dead Sea rift: Royal Society of London Philosophical Transactions, ser. A, 267, 105–127, 1970.
- Frumkin, A., Carmi, I., Zak, I., and Magaritz, M.: Middle Holocene environmental change determined from the salt caves of Mount Sedom, Israel, in: Bar-Yosef, O. and Renee S. K. (Eds.): Late Quaternary Chronology and Paleoclimates of the Eastern Mediterranean, 315–332, 1994.
- Gardosh, M., Reches, Z., and Garfunkel, Z.: Holocene tectonic deformation along the western margins of the Dead Sea, *Tectonophysics*, 180, 123–137, 1990.
- Garfunkel, Z.: Internal structure of the Dead Sea Leaky transform (rift) in relation to plate kinematics, *Tectonophysics*, 80, 81–108, 1981.
- Garfunkel, Z., Zak, I., and Freund, R.: Active faulting in the Dead Sea Rift, *Tectonophysics*, 80, 1–26, 1981.
- Gerson, R. and Grossman, S.: Later stages in the morphotectonic evolution of the southern Arava valley rift, Ministry of Energy and Infrastructure, Jerusalem. Rep. ES-1-91, 31pp, 1991.
- Ginat, H., Eyal, Y., Bartov, Y., and Zilberman, E.: Mapping of young, recent faults in the fluvial fans of Elat, *Geol. Surv. Isr. Rep.*, TR-GSI/14/94, 13pp, 1994.
- Hatzor, Y. H.: Dynamic rock slope stability analysis at Masada national monument using Block Theory and DDA, in: Amadei, B., Kranz, R., Scott, G. A., and Smeallie, P. H. (Eds.): *Rock Mechanics for industry*, Balkema, Rotterdam, 63–70, 1999.
- Hatzor, Y. H. and Levin, M.: The shear strength of clay filled bedding planes in limestones – back analysis of a slope failure in a phosphate mine, Israel, *Geological and Geotechnical Engineering*, 15, 263–282, 1997.
- Heimann, A. and Ron, H.: Young faults in the Hula pull-apart Basin, central Dead Sea Transform, *Tectonophysics*, 141, 117–124, 1987.
- Heimann, A., Zilberman, E., Amit, R., and Frieslander, U.: Yesud Hama'ala lineament – the main and young diagonal fault at the southern Hula Basin, *Geol. Soc. Isr. Annual Meeting*, Kefar Gil'adi, 45, 1997.
- Hoek, E. and Bray, J. W.: *Rock slope and Engineering*, Elsevier Applied Science, London, 358pp, 1991.
- Joffe, S. and Garfunkel, Z.: Plate kinematics of the circum Red Sea – a re-evaluation, *Tectonophysics*, 141, 5–22, 1987.
- Kadan, G.: Evidence for Dead Sea Lake-Level Fluctuations and Recent Tectonism from the Holocene Fan-Delta of Nahal Darga, Israel, Unpublished M.Sc. thesis, Ben Gurion University of the Negev (in Hebrew with English Abstract), 1997.
- Karcz, I., Kafri, U., and Meshel, Z.: Archaeological evidence for sub-recent seismic activity along the Dead Sea-Jordan rift, *Nature*, 269, 234–235, 1977.
- Kashai, E. L. and Croker, P. F.: Structural Geometry and evolution of the Dead Sea-Jordan rift system as deduced from new subsurface data, *Tectonophysics*, 141, 33–60, 1987.
- Klein, Z.: Morphological evidence of lake level changes, western shore of the Dead Sea, *Isr. J. Earth Sci.*, 31, 67–94, 1982.
- Landa, E., Shtivelman, V., and Gelchinsky, B.: A method for detection of diffracted waves on common offset sections, *Geophys. Prospecting*, 35, 359–373, 1987.
- Marco, S. and Agnon, A.: Prehistoric earthquake deformations near Massada, Dead Sea graben, *Geology*, 23, 695–698, 1995.
- Marco, S., Agnon, A., Ellenblum, R., Eidelman, A., Basson, U., and Boas, A.: 817-year old walls offset sinistrally 2.1 m by the Dead Sea Transform, Israel, *Journal of Geodynamics*, 24 (1–4), 11–20, 1997.
- Massari, F. and Colella, A.: Evolution and type of fan-delta systems in some major tectonic setting, in: Nemeč, W. and Steel, R. J. (Eds.): *Fan-deltas: sedimentology and tectonic settings*, Blackie and Son, London, 103–122, 1988.
- Miller, R. D.: Normal moveout stretch mute on shallow reflection data, *Geophysics*, V. 57, 11, 1502–1507, 1992.
- Neev, D. and Hall, J. K.: Climatic fluctuations during the Holocene as reflected by the Dead Sea levels, *International Conference on Terminal Lakes*, Ogden, Utah, 5pp, 1977.
- Niemi, T. M. and Ben-Avraham, Z.: Evidence for Jericho earthquakes from slumped sediments of the Jordan River delta in the Dead Sea, *Geology*, 22, 395–398, 1994.
- Niemi, T. M. and Ben-Avraham, Z.: Active tectonics in the Dead Sea basin, *Oxford Monographs on Geol. And Geophys.*, 36, 73–81, 1997.
- Reches, Z. and Hoexter, D. F.: Holocene seismic and tectonic activity in the Dead Sea area, *Tectonophysics*, 80, 235–254, 1981.
- Selby, M. J.: *Hill slope materials and processes*, Oxford University Press, London, 264pp, 1982.
- Shapira, A., Avni, R., and Nur, A.: A new estimate for the epicenter of the Jericho earthquake of July 11, 1927, *Isr. J. of Earth Sci.*, 42, 93–96, 1993.
- Sieh, K. E. and Jahns, R. H.: Holocene activity of the San Andreas fault at Wallace Creek, California, *Geol. Soc. Am. Bull.*, 95, 8, 883–896, 1984.
- Twiss, R. J. and Moores, E. M.: *Structural Geology*, Freeman and Company, New York, 1992.
- Zak, I. and Freund, R.: Recent strike slip movements along the Dead Sea Rift, *Isr. J. Earth Sci.*, 15, 33–37, 1966.